Reprinted from

JAPANESE JOURNAL OF
APPLIED
PHYSICS

REGULAR PAPER

Proposal of New Polishing Mechanism Based on Feret's Diameter of Contact Area between Polishing Pad and Wafer

Akira Isobe, Masatoshi Akaji, and Shuhei Kurokawa

Jpn. J. Appl. Phys. **52** (2013) 126503

© 2013 The Japan Society of Applied Physics

Person-to-person distribution (up to 10 persons) by the author only. Not permitted for publication for institutional repositories or on personal Web sites.

Japanese Journal of Applied Physics **52** (2013) 126503 **REGULAR PAPER**
http://dx.doi.org/**10.7567/JJAP.52.126503**

Proposal of New Polishing Mechanism Based on Feret's Diameter of Contact Area between Polishing Pad and Wafer

Akira Isobe[1*], Masatoshi Akaji[2], and Shuhei Kurokawa[1]

[1] *Kyushu University, Fukuoka 819-0395, Japan*
[2] *Nitta Haas Inc., Kyotanabe, Kyoto 610-0333, Japan*
E-mail: iso6016@yahoo.co.jp

Received August 1, 2013; revised September 16, 2013; accepted October 3, 2013; published online November 18, 2013

Relationships between pad surface characteristics and polishing rate are investigated. New parameter "total Feret's diameter" of contact portions is proposed as a key parameter, which shows simple correlation to the polishing rate. Feret's diameter is a projection length of a contact shape. Based on Feret's diameter, a new polishing model is proposed in which material is removed by abrasive particles existing at periphery of the pad contact portions, not on them. When a pad contact portion moves on a wafer, abrasive particles gathers at the front end of the contact portion and they remove the wafer surface material by absorbing molecules on their surface. Number of particles at contact portion is considered to be proportional to Feret's diameter. © 2013 The Japan Society of Applied Physics

1. Introduction

Chemical mechanical polishing (CMP) is widely used for leading edge electronic devices and substrates for them such as large scale integrated (LSI), Si wafer, glass or aluminum substrates for hard disk drive or sapphire wafer for light emission diode (LED).[1–7] However, its fundamental mechanism for material removal has not been clarified yet. Therefore, optimization of the CMP conditions or development of the consumable materials still relies on "experience" and "try and error". The reason why it is difficult to understand the mechanism of CMP is because CMP has various parameters and they affect each other. For example, friction increases temperature during polishing, the increased temperature changes pad property and the pad property affect the friction. We need to investigate CMP phenomena carefully and need to separate these factors independently to find out key parameters. At this moment, parameters which can be measured easily, such as pad hardness, density, slurry particle size or its distribution are used to see the dependencies to removal rate (RR) and these dependencies are applied for process optimizations. However, such dependencies may show quite opposite behavior in another circumstance. It means that the parameter is not the key parameter and the dependencies are not based on direct relationship between the parameters and the RR. We need to consider the mechanism of the relationship between the parameters and the RR, otherwise, we may be trapped by a superstition.

Here, we look back studies for polishing mechanism. RR is known to follow Preston's equation.[8] It is an empirical equation which indicates that RR is proportional to wafer pressure as well as relative speed between polishing pad and wafer. There are several models which explain why RR is proportional to wafer pressure. Izumitani proposed a model in which glass surface is softened by chemical factor and the softened layer is removed by mechanical factor.[9] Based on this concept, Cook showed a model where particles in the slurry are indented into the glass surface and RR is determined by the indentation depth.[10] The volume of the groove created by the indentation is proportional to the relative velocity and the force to an abrasive particle. Therefore RR is proportional to the pressure and the speed. He considered all the down force is applied to the particles. He considered the pad surface flat and the number of the particle on the pad can be calculated with the particle size, the particle concentration and a "filling factor". Therefore, the particle pressure is proportional to the wafer pressure in this model because the number of working particles is constant.

At that time, a concept of real contact area was not known and Cook considered total area of the pad works for polishing. In 1995, Mitsuhashi et al. measured real contact area of a polishing pad to a wafer surface using the most popular polishing pad, IC1000, pressed onto a glass. They found that the contact area between the polishing pad and the wafer was very small, 1% or less, and it is proportional to the wafer pressure.[11] These results are now accepted widely and many other studies have been presented after that.[12–16] Based on this, some models were proposed.

Qin indicated that the pad contact area is proportional to the wafer pressure by solving theoretical equations based on Greenwood–Williamson model.[15] Then he explained that the particle pressures could not be changed by the wafer pressure because the average pressure for the pad contact area should be constant. Qin considered that the wafer pressure dependency to the RR is caused by the change of the pad contact area. Number of the working particle is dependent on the contact area and it is the cause of the RR dependency on the wafer pressure in his model. He still considered there is a gap between pad surface and the wafer surface by existing of particles and the all force to the wafer is transferred to the particles. Luo proposed a model in which the particles are embedded on the pad contact areas.[16,17] Choi evaluated polishing rate and the wafer surface roughness after polishing by changing the wafer pressure, particle size and its concentration in a slurry.[18] It was confirmed that RR is proportional to the wafer pressure but surface roughness was constant even with different wafer pressures when the particle size is the same. This result seems to support Qin's model. However, when the particle concentration was changed, surface roughness did not change. If the wafer pressure is entirely transferred to particles, the force per particle must be decreased when the number of the particle is increased. Choi considered that the particles are embedded in the pad surface and most of the wafer pressure is supported by the pad surface. This result supports Luo's model.

 © 2013 The Japan Society of Applied Physics

Person-to-person distribution (up to 10 persons) by the author only. Not permitted for publication for institutional repositories or on personal Web sites.

The conclusions of Refs. 15–18, however, are the same that material removal is carried out by indentation of particles existing at pad contact pinched between the pad surface and the wafer surface. The number of particles at contact area is the key for their models. They considered that change of the number by the wafer down force is the cause of the pressure dependency in Preston's equation. After that, modified models were proposed by many researchers but all those models consider abrasive particles on pad asperity tips work for the material removal.[19–22)]

A question arises. The above models consider that the number of abrasive particle is proportional to the contact area, but can particles exist on pad contact area uniformly? It seems difficult to be there because the particles may be scraped by the wafer. Then, there must be an effect of the contact size or its shape. This paper investigates various contact parameters to find the key parameter of the contact area to polishing rate. From the result, a new model for polishing mechanism is proposed.

2. Experimental Procedure

Polishing pad's surface condition is known to be varied with polishing itself without dressing, especially for silicon oxide polishing.[23–25)] Abrasive particles in a slurry also polish pad surface to cause this phenomenon. Thus, it is difficult to evaluate the relationship between the pad surface property and the RR in such an unstable condition. We selected tungsten CMP for the evaluation because its mechanical effect to the polishing pad surface is known to be much smaller than silicon oxide CMP because of much lower concentration of abrasives in the tungsten slurry. It is known that the tungsten surface is oxidized by a slurry and the oxidized layer is mechanically removed by abrasive particles in the slurry.[26,27)] Oxidizing is a chemical factor but it is considered to be constant in this evaluation because CMP process conditions are the same. Then, we can evaluate mechanical factors by this evaluation without the influence of pad surface change during polishing.

IC1400™ from Nitta Haas was used as a polishing pad. Four different surface pads were prepared by using buffing with different mesh sizes of buffing sheet. Figure 1 shows the surface photos of the pads. The pad surface roughness was measured using a laser microscope Keyence VK-9700. R_a, R_p, R_v, and R_z were calculated as the parameters of roughness. Contact area was evaluated by pressing a sapphire glass onto the pad with 35 kPa, which is the same pressure used in CMP test, as shown in Fig. 2. Measured area size was $1.04 \times 1.38\,\text{mm}^2$. The observed images were processed to obtain contact area, contact number and Feret's diameter. "Feret's diameter" means the rectangular length circumscribing to a contact portion, as shown in Fig. 3. The total Feret's diameter (F) can be expressed as Eq. (1). Here, f_n represents the Feret's diameter of each contact portion:

$$F = \sum f_n. \tag{1}$$

CMP test was performed with an Ebara EPO-222. A Cabot SSW-2000 was used as a slurry and was diluted 2 times with deionized water. H_2O_2 was used as an oxidizer and its concentration was 2 wt%. Abrasive particle concentration was 6% in original slurry and becomes less than 3% at point of use (POU), which is much lower than standard oxide slurry's 12.5%.

Polishing conditions are as follows. Wafer pressure was 35 kPa, rotation speeds for head and platen were 120 and 119 min^{-1}, respectively, slurry flow rate was 125 ml/min and polishing time was 60 s. 200 mm tungsten wafers were polished, on which 0.8 μm thermal CVD tungsten was deposited on SiO_2 and TiN. Four-probe method was applied

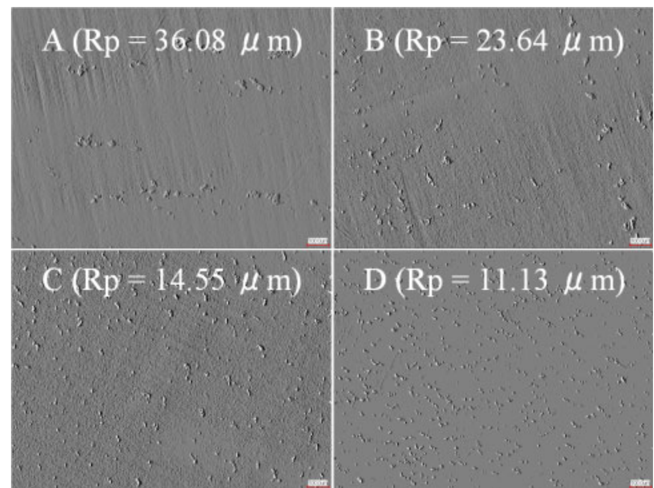

Fig. 1. (Color online) Optical image of contact area for four different surface pads.

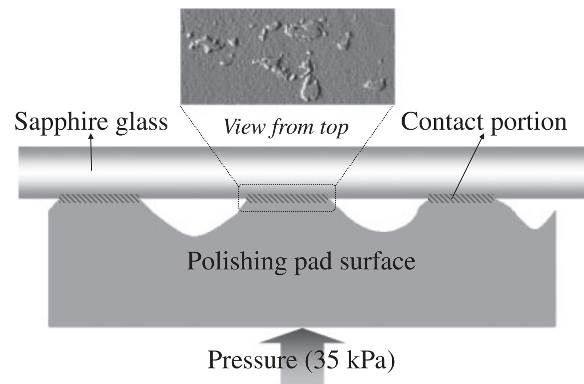

Fig. 2. Measurement of pad contact.

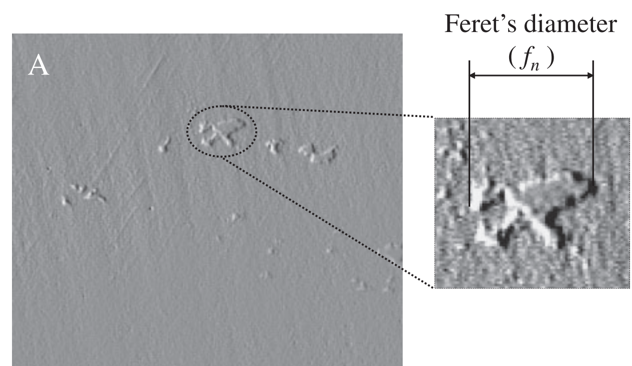

Fig. 3. Feret's diameter of a contact area.

© 2013 The Japan Society of Applied Physics

Person-to-person distribution (up to 10 persons) by the author only. Not permitted for publication for institutional repositories or on personal Web sites.

Table I. Pad surface roughness (in μm).

	R_p	R_v	R_z	R_a
Pad A	36.07	13.50	49.41	8.38
Pad B	23.64	8.04	31.79	5.04
Pad C	14.55	4.08	18.64	2.82
Pad D	11.13	3.24	14.37	2.44

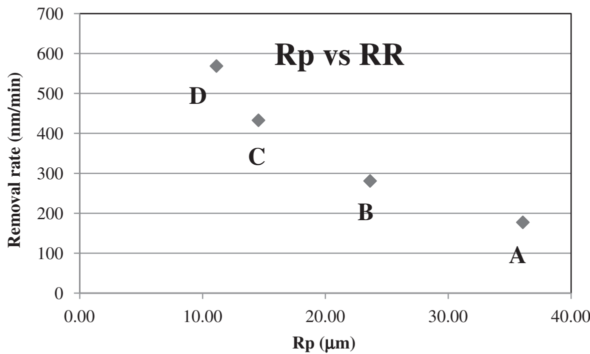

Fig. 4. Polishing rate vs R_p of polishing pads.

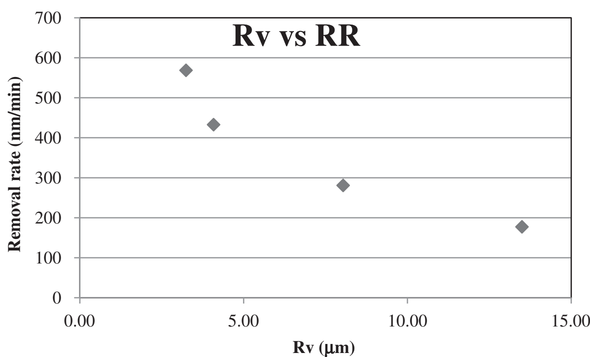

Fig. 5. Polishing rate vs R_v of polishing pads.

to measure the thickness of the tungsten before and after polishing to evaluate the RR.

3. Results

Pad surface evaluation results are summarized in Table I. Figures 4 to 7 show the relationship between pad surface roughness parameters and the RR. Figure 4 shows the relationship between R_p and the RR. Higher R_p pad shows lower RR but the relationship between R_p and RR does not seem simple. The other roughness parameter, R_a, R_v, and R_z, shows similar behavior as R_p. In general, those parameters cannot be a key parameter for polishing because wave length of the roughness is not considered in the parameters. Roughness shown in Figs. 8(a) and 8(b) are both expressed with the same R_a or R_p. Khajornrugang proposed to use power spectrum of surface roughness for roughness evaluation[28] but still roughness cannot be the direct parameter. When we consider that the material removal occurs at the pad contact portion in polishing, parameters related to contact area should be more direct. Surface roughness, of course, affects the pad contact, therefore pad roughness

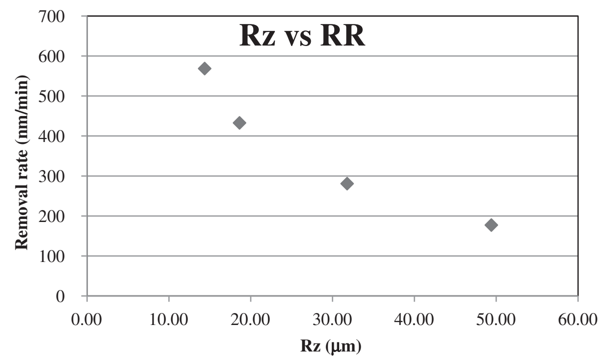

Fig. 6. Polishing rate vs R_z of polishing pads.

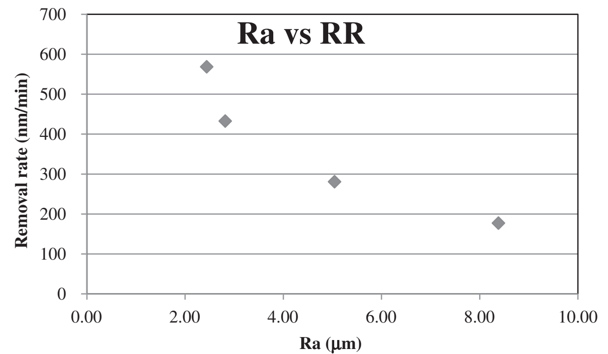

Fig. 7. Polishing rate vs R_a of polishing pads.

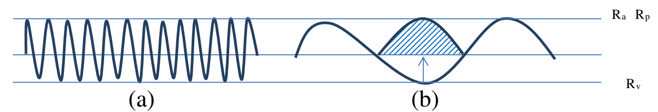

Fig. 8. (Color online) Illustration of roughness, (a) and (b) show the same R_a, R_p, and R_v.

Table II. Measured contact area parameters in 1 mm^2 of polishing pad surface.

	Number of contact portion	Contact area (μm^2)	Total Feret's diameter (μm)
Pad A	118	1078	9252
Pad B	261	2564	26261
Pad C	474	4438	41398
Pad D	525	5764	45688

looks to have impact to the RR but it should be considered to be indirect parameter.

Measured parameters related to contact area are listed in Table II. Figure 9 shows the relationship between polishing rate and contact area. Here, the contact area is defined as the contact area (μm^2) in 1 mm^2 area. Definitions for following parameters are the same. A pad with higher contact area shows higher RR. However, the relationship is not linear. Figure 10 shows the relationship between the RR and the number of contact portion. Here, the higher number of

 © 2013 The Japan Society of Applied Physics

Person-to-person distribution (up to 10 persons) by the author only. Not permitted for publication for institutional repositories or on personal Web sites.

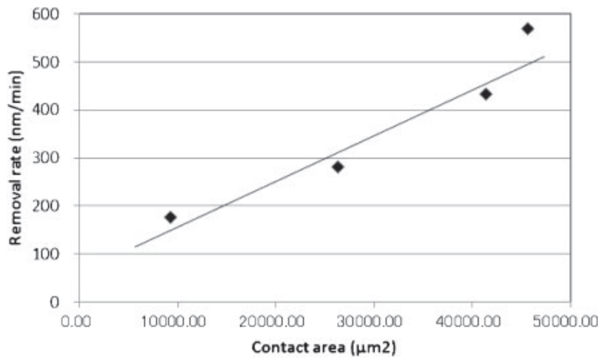

Fig. 9. Polishing rate vs number of contact portions of polishing pad.

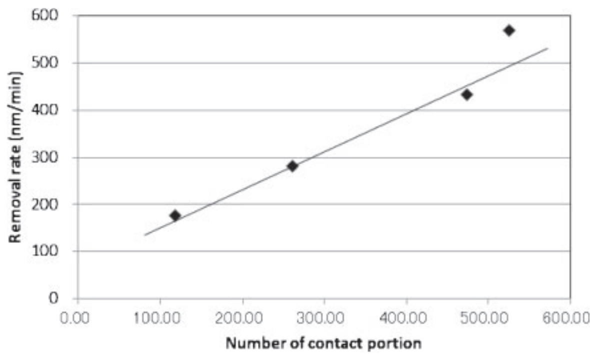

Fig. 10. Polishing rate vs contact area of polishing pad.

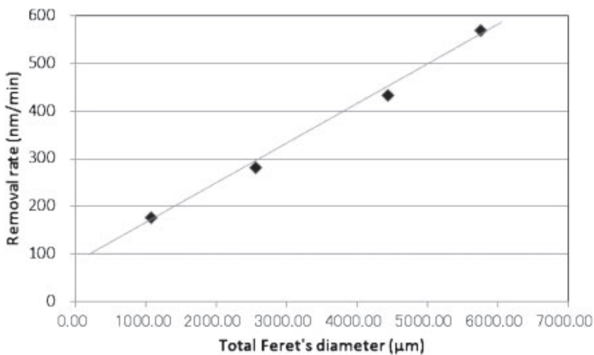

Fig. 11. Polishing rate vs total Feret's diameter of contact portions.

contact portion shows higher RR as similar as contact area case but it is not linear either. Finally, the relationship between total Feret's diameter and the RR is shown in Fig. 11. Four plots are almost on a line.

4. Discussion

The meaning of the strong correlation between the total Feret's diameter and the RR is considered here. Qin and Choi considered that the pad contact area is proportional to the wafer pressure and that the working particles increase with the contact area resulting in the higher RR. However, we did not confirm the linearity of polishing rate with the pad contact area. Their model is based on the hypothesis that particles exist on pad contact area uniformly and the number of the particle is proportional to the contact area. However, it

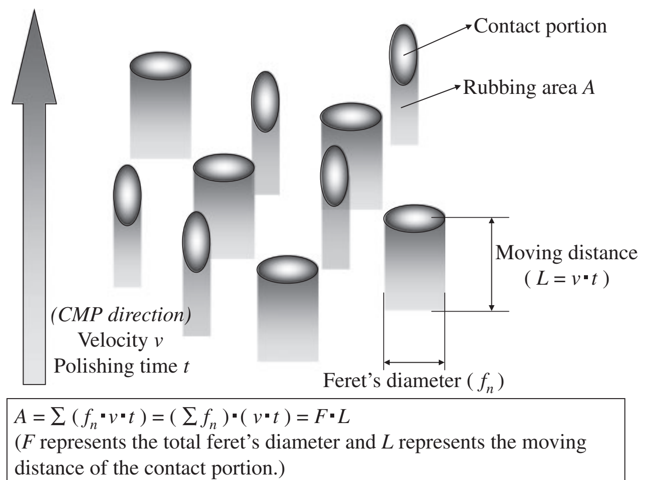

$A = \sum (f_n \cdot v \cdot t) = (\sum f_n) \cdot (v \cdot t) = F \cdot L$
(F represents the total feret's diameter and L represents the moving distance of the contact portion.)

Fig. 12. Illustration for traces of contact portions.

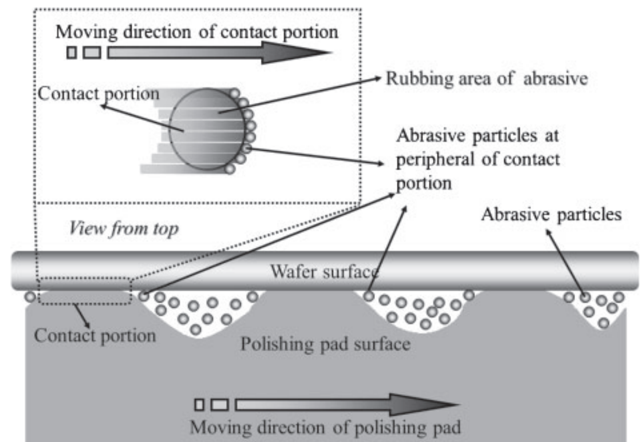

Fig. 13. Illustration showing the concept of the model.

is difficult to consider many particles exist uniformly on the pad contact area pinched with wafer surface. Recently, many studies have been reported which analyze the particle motion in a slurry by simulation or observing it directly.[29,30] However, there is no report which confirms transported particles stay between a pad contact portion and wafer surface. It is reasonable to consider that particles move in liquid and some of them are stacked at peripheries of a pad contact. The number of stacked particle is considered to be proportional to the size of the contact portion. Here, the parameter of the contact "size" should not be the contact area but the Feret's diameter. Figure 12 is an illustration for traces of pad contact portions. The area of the traces of the contact portions are expressed by Feret's diameter and the travel length for unit time, which means the relative speed. The abrasive particles in a slurry are considered to be stacked at the leading edge of peripheries of contact portions as shown in Fig. 13. Material removal is considered to be carried out by absorbing molecules from the wafer surface onto the particle surface.[31,32)]

We showed that there is a linearity between the total Feret's diameter and the RR, but when the line is extended it crosses with y-axis at around 100 nm/min. It can be

 © 2013 The Japan Society of Applied Physics

Person-to-person distribution (up to 10 persons) by the author only. Not permitted for publication for institutional repositories or on personal Web sites.

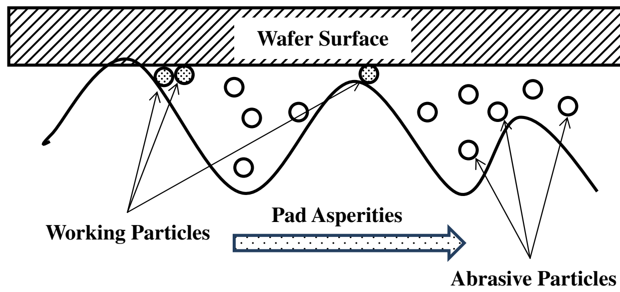

Fig. 14. (Color online) Illustration showing abrasive particles between the wafer surface and the pad asperities.

considered as shown in Fig. 14. Particles can stack even when pad surface is not contacted to wafer surface if the distance is below the particle size. This effect can explain the bias of the RR.

Finally, we consider whether this model can explain the RR dependency on wafer pressure. When the contact number is constant, total contact area is proportional to the wafer pressure and total Feret's diameter is proportional to (wafer pressure)$^{1/2}$. However, when wafer pressure increases, new contact portions appear and they must be small. We calculated the relationship between total Feret's diameter and total contact area. Mitsuhashi reported that the contact area is proportional to wafer pressure and Qin confirmed this relationship by equations. In his paper, contact area was expressed by Eq. (2) and force to wafer was expressed by Eq. (3):

$$A = \pi N A_0 \beta \int_h^{\infty} (z - h)\varphi(z)\,dz, \quad (2)$$

$$\mathrm{L} = \frac{4}{3} N A_0 E^* \beta^{1/2} \int_h^{\infty} (z - h)^{3/2}\varphi(z)\,dz. \quad (3)$$

Here N is the number density of the pad asperities (i.e., number of asperities per unit platform area), A_0 is the total area of the flat wafer surface, β is the mean radius of curvature of the tip of the pad asperities, h is the average gap between the smooth wafer and the rough pad under the given conditions, φ is the distribution function for the height of the asperities. E^* is the composite modules between the two surfaces in contact that is defined as

$$\frac{1}{E^*} = \frac{1 - \nu_{\mathrm{p}}^2}{E_{\mathrm{p}}} + \frac{1 - \nu_{\mathrm{w}}^2}{E_{\mathrm{w}}}. \quad (4)$$

Here E and ν are the Young's modulus and the Poisson's ratio, and the subscripts p and w represent the pad and the wafer, respectively.

Applying normal distribution Eq. (5) to Eqs. (2) and (3), he concluded that contact area is proportional to wafer pressure:

$$\varphi(z) = \frac{1}{\sigma\sqrt{2\pi}} \exp\left(-\frac{z^2}{2\sigma^2}\right). \quad (5)$$

Here σ is the standard deviation of the pad asperity heights. If we show the linear relationship between Feret's diameter and contact area, it means Feret's diameter is proportional to wafer pressure and it can be the explanation of polishing rate dependency on wafer pressure. Now, total Feret's diameter F can be written as

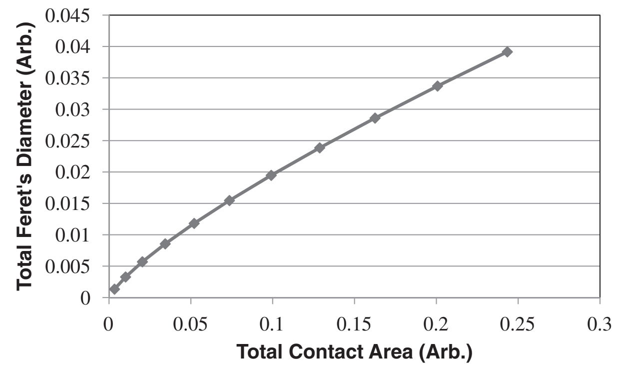

Fig. 15. Relationship between calculated total contact area vs calculated total Feret's diameter.

$$F = 2NA_0\beta^{1/2} \int_h^{\infty} (z - h)^{1/2}\varphi(z)\,dz. \quad (6)$$

The integral cannot be obtained but numerical integration was calculated. The input values are, 10 µm for σ, 25 µm for β, and 25 µm for pad top surface height, respectively. The relationship between Feret's diameter and contact area is plotted in Fig. 15. It shows almost linear relationship. Since contact area is proportional to wafer pressure, x-axis of the figure can be converted to wafer pressure. That is, Feret's diameter has almost linear relationship to wafer pressure. It suggests that Feret's diameter can explain the wafer pressure dependency of RR in Preston's equation. The curve shows a little bit superlinear but this trend has been reported in many papers. There is a possibility that this model can explain actual polishing behaviors more precisely. Note that this relationship between contact area and total Feret's diameter is only for a fixed roughness pad surface. Therefore, it does not conflict the results of Figs. 9 or 10.

5. Conclusion

Total Feret's diameter showed strong correlation to RR and was considered to be a key parameter which directly affect the RR. A model of polishing was proposed where particles in slurry are stacked at contact portion and the number of particle is determined by Feret's diameter. This new model will help to develop new consumables such as polishing pads which can gather more particles at contact area or slurries which have particle size distribution optimized for maximizing the particle number at pad contact portions.

1) A. Isobe: Proc. SEMI Technology Symp. Japan, 1991, p. 276.
2) M. Krishnan, J. W. Nalaskowski, and L. M. Cook: Chem. Rev. **110** (2010) 178.
3) Y. Moon, R. Venigalla, C. Sheraw, C. Wang, J. Cummings, D. Canaperi, D. Lee, L. Hall, and L. Economikos: Proc. ICPT, 2009, p. 183.
4) W. J. Patrick, W. L. Guthrie, C. L. Standley, and P. M. Schiable: J. Electrochem. Soc. **138** (1991) 1778.
5) S.-Y. Kim and Y.-J. Seo: Microelectron. Eng. **60** (2002) 357.
6) H.-P. Feng, J.-Y. Lin, M.-Y. Cheng, Y.-Y. Wang, and C.-C. Wan: J. Electrochem. Soc. **155** (2008) H21.
7) Z.-C. Lin, W.-S. Huang, and J.-S. Tsai: J. Mech. Sci. Technol. **26** (2012) 2353.
8) F. Preston: J. Soc. Glass Technol. **11** (1927) 127.
9) T. Izumitani: Treatise Mater. Sci. Technol. **17** (1979) 115.
10) L. M. Cook: J. Non-Cryst. Solids **120** (1990) 152.

 © 2013 The Japan Society of Applied Physics

Person-to-person distribution (up to 10 persons) by the author only. Not permitted for publication for institutional repositories or on personal Web sites.

11) M. Mitsuhashi, H. Ono, and A. Isobe: Proc. JSPE Fall Meet., 1995, p. 20 [in Japanese].
12) C. L. Elmufdi and G. P. Muldowney: MRS Proc. **914** (2006) 0914-F12-06.
13) L. J. Borucki, T. Sun, Y. Zhuang, D. Slutz, and A. Philipossian: MRS Proc. **1157** (2009) 1157-E01-02.
14) M. Uneda, Y. Maeda, K. Ishikawa, K. Ichikawa, T. Doi, T. Yamazaki, and H. Aida: J. Electrochem. Soc. **159** (2012) H90.
15) K. Qin, B. Moudgil, and C.-W. Park: Thin Solid Films **446** (2004) 277.
16) J. Luo and D. A. Dornfeld: IEEE Trans. Semicond. Manuf. **14** (2001) 112.
17) J. Luo and D. A. Dornfeld: J. Electrochem. Soc. **150** (2003) G807.
18) W. Choi and R. K. Singh: Jpn. J. Appl. Phys. **44** (2005) 8383.
19) Y.-R. Jeng and P.-Y. Huang: Electrochem. Solid-State Lett. **7** (2004) G40.
20) J. Seok, C. P. Sukam, A. T. Kim, J. A. Tichy, and T. S. Cale: Wear **254** (2003) 307.
21) G. Fu, A. Chandra, S. Guha, and G. Subhash: IEEE Trans. Semicond. Manuf. **14** (2001) 406.
22) J. Xin, W. Cai, and J. A. Tichy: Wear **268** (2010) 837.
23) D. Stein, D. Hetherington, M. Dugger, and T. Stout: J. Electron. Mater. **25** (1996) 1623.
24) T. Fujita, M. Ishikura, N. Kawai, and Y. Morioka: Seimitsu Kogaku Kaishi **74** (2008) 815 [in Japanese].
25) S. A. Lawing: presented at SEMI Technol. Symp. SEMICON China, 2004.
26) E. A. Kneer: J. Electrochem. Soc. **144** (1997) 3041.
27) S. Ojima, T. Funakoshi, T. Hori, M. Abe, and T. Doi: Proc. Pacrim CMP, 2004, p. 234.
28) P. Khajornrungruang, K. Kimura, T. Okuzono, K. Suzuki, and T. Kushida: Jpn. J. Appl. Phys. **51** (2012) 05EF04.
29) E. J. Terrell and C. F. Higgs, III: J. Tribology **129** (2007) 933.
30) G. P. Muldowney and D. P. Tselepidakis: presented at CMPMIC, 2004.
31) K. Kimura: presented at Levitronix Users Conf., 2011.
32) R. Burtovyy, Y. Liu, B. Zdyrko, A. Tregub, M. Moinpour, M. Buehler, and I. Luzinov: J. Electrochem. Soc. **154** (2007) H476.

© 2013 The Japan Society of Applied Physics